ChemComm

Accepted Manuscript

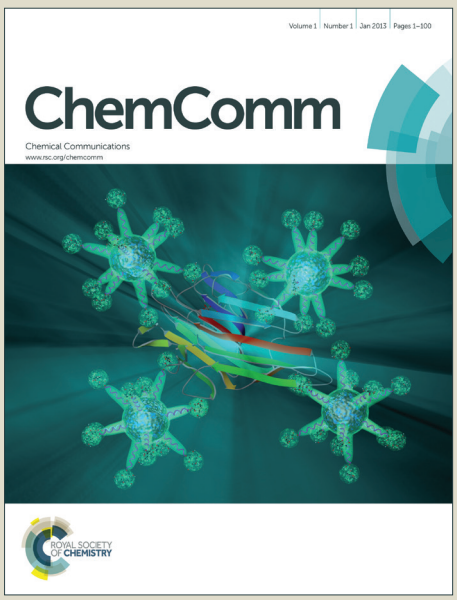

ROYAL SOCIETY OF CHEMISTRY

www.rsc.org/chemcomm

Journal Name

RSCPublishing

COMMUNICATION

Pendant ionic groups of conjugated oligoelectrolytes govern their ability to intercalate into microbial membranes

Cite this: DOI: 10.1039/x0xx00000x

Received 00th January 2012,
Accepted 00th January 2012

DOI: 10.1039/x0xx00000x

www.rsc.org/

A. W. Thomas,[a] C. Catania,[b] L. E. Garner[c] and G. C. Bazan[a,b]

Conjugated oligoelectrolytes (COEs) bearing pyridinium and carboxylate groups are synthesized, characterized, and compared to the trimethylammonium analogue from which they are derived. All COEs are able to spontaneously intercalate into liposomes, whereas only positively charged COEs intercalate into *E. coli* membranes. Membrane intercalation is determined necessary for performance enhancement in microbial fuel cells.

Lipid bilayers are found ubiquitously in nature, constituting the semipermeable barrier separating biological cells from their surroundings and forming a dynamic scaffold for the intricate organization of proteins in complex metabolic reactions. Modifying this pervasive interface through synthetic constructs is a challenging task with enormous potential for therapeutics, industrial applications and basic science.[1] With this intention, many complex molecular and supramolecular structures have been synthesized as synthetic ion channels[2-4] or transmembrane electron transporters[5-8] with structural motifs facilitating the passage of charged species through the hydrophobic bilayer core.

Conjugated oligoelectrolytes (COEs) are water-soluble molecules with π-conjugated backbones bearing pendant ionic groups. Certain conjugated oligoelectrolytes (COEs) have attracted attention for their ability to spontaneously intercalate into lipid bilayers and, in turn, modify the membrane transport properties.[9] This modification has been shown to boost the performance of a variety of microbial bioelectronic devices.[10-12] This technology relies on overcoming the electronically insulating character of lipid membranes in order to link intracellular metabolism to extracellular electronics; a feat that few bacteria are naturally able to do.[13] Although the mechanism by which COEs improve bioelectronic interactions may be situation dependent,[14-16] their ability to favorably modify the microbe-electrode interface[17] through spontaneous intercalation into lipid membranes is presumed paramount to their function.

A number of COE structural modifications have been studied and proven consequential to their biological interactions. Molecular length affected both mammalian membrane patch stability in ion conduction experiments[15] and microbial toxicity,[18] where a bolaamphiphilic, phenylenevinylene COE, **DSSN+** (Scheme 1), is thought to more closely match the width of lipid bilayers and consequently provided more membrane stability and lower toxicity when compared to shorter and longer analogues. Furthermore, molecular topology, particularly the spatial distribution of the solubilizing ionic groups, impacts COE-membrane interactions and thus potential applications.[19,20]

In this contribution we take advantage of synthetic flexibility to access three COEs through simple one- or two-step procedures from a common starting material in order to understand of the effect of different pendant ionic groups on membrane and bioelectronic interactions. Specifically, the trimethylammonium groups of **DSSN+** were substituted with either aromatic cationic pyridinium groups or anionic carboxylate groups to provide **DSSNpyr** and **DSSNcarb** (see Scheme 1 for chemical compositions). As described in more detail below, we find remarkable selective interactions that are tuned to the choice of charge within the COE structure.

Scheme 1 provides a summary of the synthetic route for the preparation of the new COEs. Complete details can be found in the Supporting Information. The synthesis of **DSSN+** has been reported previously.[9] Starting from the tetraiodo-substituted precursor of **DSSN+** (compound **1**), **DSSNpyr** is obtained via quaternization with

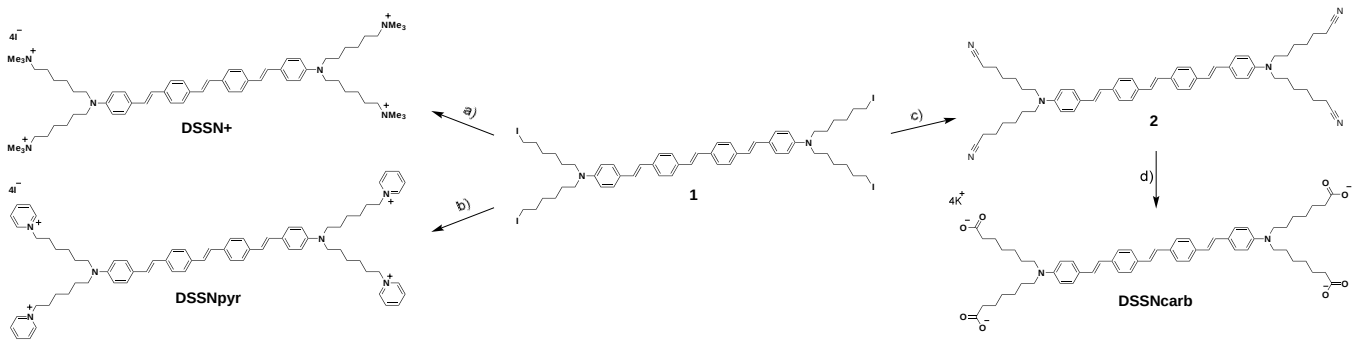

Scheme 1 Synthesis of the COEs used in this study. Reagents and conditions: a) NMe3, THF, MeOH; b) pyridine (neat); c) KCN, 18-crown-6, MeCN; d) KOH, H2O, MeOH, 150 °C (microwave).

pyridine. In a two-step process, **1** is treated with potassium cyanide to obtain a tetracyano-substituted intermediated (compound **2**) which is then hydrolyzed under basic conditions to yield the tetracarboxylated derivative **DSSNcarb**.

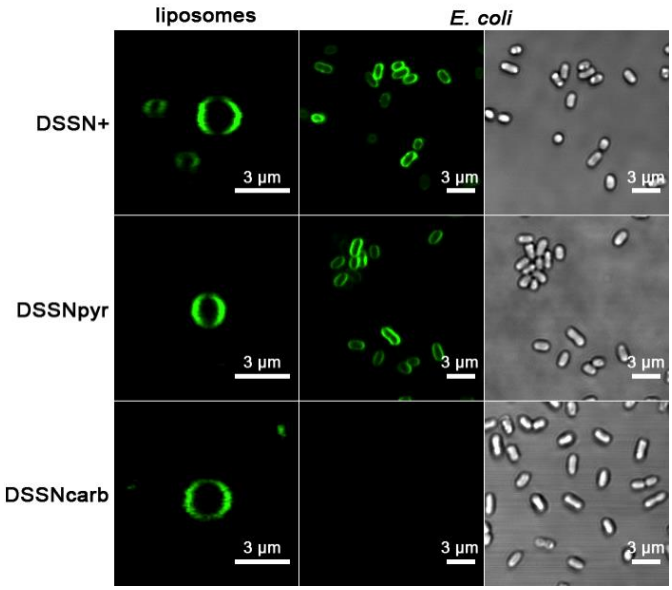

Fig. 1. Confocal micrographs of *E. coli* lipid extract liposomes (left column) stained with 1 mol% COE based on lipid concentration and live *E. coli* cells (middle column) stained with 10 μM COE. Corresponding brightfield images of *E. coli* are shown (right column). Laser excitation was at 405 nm with emission collected 480 – 580 nm.

Liposomes composed of *E. coli* lipid extract were used as model membranes to compare the intercalating abilities of **DSSN+**, **DSSNpyr**, and **DSSNcarb**. In this experiment, COEs were added extraneously via concentrated aqueous solution to pre-formed liposomes in buffer. Aliquots were subsequently imaged via laser scanning confocal microscopy by direct excitation of the COE conjugated core. As seen in Fig. 1, all COEs display circular emission profiles with negligible background emission, consistent with liposome incorporation and an environmentally sensitive fluorescence quantum efficiency.[9] Large liposomes (1–2 μm diameter) revealed uneven emission profiles characteristic of ordered orientation within the lipid bilayer. Specifically, the emission profiles become less intense along the vertical axis and more intense along the horizontal axis due to the varying interaction between the transition dipole of the COE chromophore and the inherently polarized excitation laser. [9,21] This anisotropy in all three cases confirms their ability to predominantly span the lipid bilayer with the long axis of the molecule parallel with the lipid tails. Finally, emission from all COEs was observed in multiple layers of multilamellar liposomes (see Fig. S1), suggesting that they are able to traverse a lipid bilayer. In the end, changing the ionic pendant groups of these COEs has no observable effect on liposome incorporation under the experimental conditions described here.

Turning from model membranes to *in vivo* interactions, *E. coli* cells were stained and the results are shown in Fig. 1. The cationic COEs (**DSSN+** and **DSSNpyr**) successfully intercalated into the cell membranes, as evidenced by their emission profiles associated with the edges of the cells. In contrast, **DSSNcarb** gave no detectable emission, indicating that the anionic COE remained in solution. Considering that **DSSNcarb** can intercalate into liposomes of *E. coli* lipids but cannot intercalate into the membranes of *E. coli* cells, a previously unconsidered interaction must be governing the ability of COEs to intercalate into cell membranes. This interaction is most reasonably assumed to be with the anionic lipopolysaccharide (LPS) layer surrounding the outer membrane of *E. coli* and most gram-negative bacteria;[22] a feature that gives these cells a negative surface charge and has been exploited for electrostatic interactions with oligo- and polyelectrolytes.[23-28] Under these circumstances, electrostatic attraction and repulsion of LPS with cationic and anionic COEs, respectively, provides the means for gating membrane intercalation.

As discussed in the introduction, **DSSN+** has been shown to improve the performance of microbial fuel cells (MFCs) when added in concentrations ≥ 10 μM.[29] **DSSNpyr** and **DSSNcarb** were therefore compared with **DSSN+** and a control with no-COE using two-chamber U-tube MFCs[30,31] employing *E. coli* as the biocatalyst and Luria broth as the organic fuel. In these devices, microbes oxidize organic matter in the anaerobic anode chamber releasing CO_2, protons and electrons, the later of which can be collected at the anode electrode. Completing the circuit is the cathode reaction that combines protons, electrons and O_2 to form water in a chamber that is separated by a proton exchange membrane and open to air.[32]

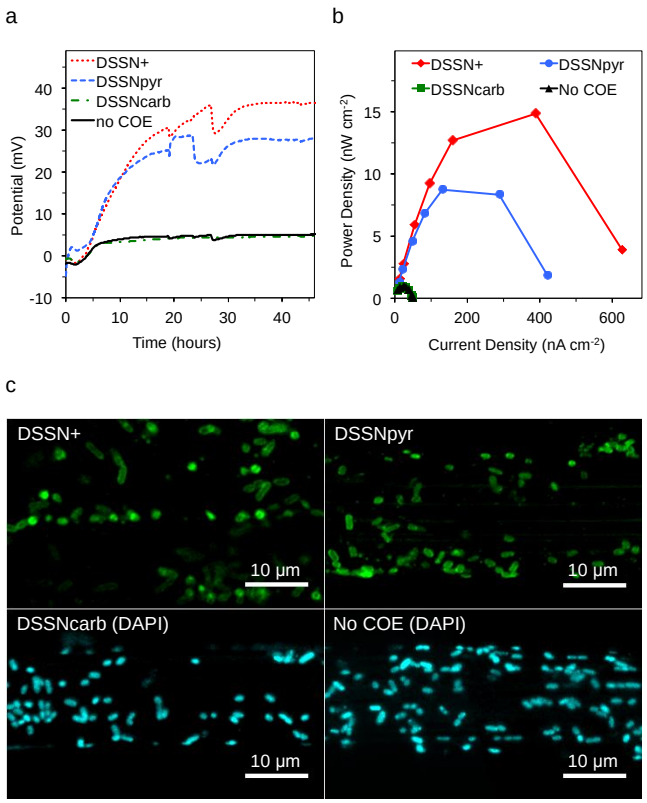

Fig. 2. (a) Average potential generation over 46 hours of triplicate *E. coli* MFCs run with 0 or 10 µM of the three COEs. Sharp spikes in data result from the dislodging of CO_2 bubbles formed in the anode chamber by *E. coli.* (b) Average power generation of each set of triplicate devices obtained after 46 hours of operation. (c) Representative confocal micrographs of graphite felt fibers from the MFC anodes after operation. No emission was detected for **DSSNcarb** or no-COE electrode fibers (images not shown) prior to staining with 5 µM DAPI. Laser excitation was at 405 nm with emission collected 500 – 600 nm and 420 – 520 nm for COEs and DAPI, respectively.

COEs were added to the MFC anaerobic anode chambers to a final concentration of 10 µM prior to inoculation with an overnight culture of *E. coli* to an optical density of 0.1 (OD_{600nm}). The addition of 10 µM COEs did not significantly affect *E. coli* growth in a separate experiment (Fig. S2). The potential across a 10 kΩ resistor was monitored for 46 hours. Graphite felt served as the electrode material. Fig. 2A shows the voltage generated over time for the MFCs, reported as an average of triplicate devices for each condition. The first noteworthy observation is that devices run with **DSSNcarb** performed nearly identically to no-COE controls, with both reaching a maximum sustained average potentials of approximately 4.5 mV after ~33 hours. **DSSN+** and **DSSNpyr** devices exhibited greater than 6-fold improvement over the control as shown by the corresponding maxima of 36 mV and 28 mV, respectively.

At the end of MFC operation shown in Fig. 2A, power density curves were obtained for each device by varying the resistance between the anode and cathode and measuring the voltage once it stabilized (~20 minutes). The results of this experiment are shown in Fig. 2B. One observes that devices run with **DSSN+** and **DSSNpyr** gave greater than 9-fold improvement with maximum power densities of ~15 nW cm^{-2} and ~9 nW cm^{-2}, respectively. The control devices and **DSSNcarb** led to maximum power densities of less than 1 nW cm^{-2}. These experiments, together with those in Fig. 2A, show that while the synthetic change from trimethylammonium to pyridinium slightly decreased MFC performance, the change to a negatively charged carboxylate completely eliminated any performance enhancement under these experimental conditions.

As a final examination after MFC operation, carbon felt anode electrodes from the devices were compared by confocal microscopy and representative images are shown in Fig. 2C. In the case of **DSSN+** and **DSSNpyr**, no additional dyes were added; therefore, any resulting emission is from COEs present at the start of operation. **DSSN+** and **DSSNpyr** electrodes displayed emission patterns consistent with COEs incorporated into *E. coli* cells: the patterns comprised mostly of short rod-shaped objects ~2 µm by ~0.5 µm, comparable to the *E. coli* in Fig. 1. The **DSSNcarb** and no-COE electrodes gave no emission under identical settings (images not shown). In order to determine if cells were attached to these electrodes they were stained with 5 µM DAPI, a nucleic acid stain; representative images are shown in the bottom row of Fig. 2C. Both **DSSNcarb** and no-COE electrodes exhibit cell attachment to the graphite felt fibers via DAPI staining, indicating that **DSSNcarb** was not inhibiting cell attachment. Comparing all four MFC conditions, electrode coverage by *E. coli* is similar. Additionally, DAPI staining of **DSSN+** and **DSSNpyr** device electrodes (Fig. S3) showed that all cells displaying DAPI emission also displayed COE emission, suggesting that all cells on the electrode have COEs incorporated. These results suggest a direct correlation between COE membrane intercalation and increased voltage and power generation in MFCs under these experimental conditions.

Conclusions

In conclusion, two novel COEs were synthesized based on the membrane intercalating **DSSN+** by changing its pendant ionic groups from trimethylammonium to either pyridinium (**DSSNpyr**) or carboxylate (**DSSNcarb**). Based on confocal microscopy, **DSSN+**, **DSSNpyr** and **DSSNcarb** can be classified as membrane intercalating due to their ability to spontaneously intercalate into liposomes composed of *E. coli* lipid extract. We have determined, however, that this attribute does not necessarily impart the ability to incorporate into the membranes of live *E. coli*, as **DSSNcarb** was unable to do so. Additional cell surface components must participate in preventing this anionic COE from penetrating into the membrane, and we propose that the anionic LPS content in *E. coli* may be playing an important role in this charge selectivity.[22] We surmise that hydrophobic interactions between the molecular core of COEs and lipid tails play a role in the ability of COEs to persist within a membrane as evidenced by the inability of a cationic COE with a more hydrophilic core to intercalate and remain in biological membranes,[19] but that electrostatic interactions first govern intercalation. Furthermore, both cationic COEs were able to incorporate into *E. coli* membranes and improved the performance of *E. coli* MFCs, while **DSSNcarb** did not. This suggests that there is a direct correlation between a COE's ability to intercalate into membranes and its ability to improve MFC performance. Information

gained from this study will expand a growing collection of synthetic design rules for biologically relevant COEs that are finding utility in bioelectrochemical devices as well as biological detection[33-36] and imaging applications.[37-38]

This work was supported by the Institute for Collaborative Biotechnologies through grant W911NF-09-0001 from the U.S. Army Research Office.

Notes and references

[a] Center for Polymers and Organic Solids, Department of Chemistry and Biochemistry, University of California, Santa Barbara, CA 93106, USA
E-mail: bazan@chem.ucsb.edu

[b] Materials Department, University of California, Santa Barbara, CA 93106, USA

[c] National Renewable Energy Laboratory, 15013 Denver W Pkwy, Golden, CO 80401,USA

Electronic Supplementary Information (ESI) available: Synthetic procedures, experimental details, and additional confocal images. See DOI: 10.1039/c000000x/

1 S. Matile, T. Fyles, *Acc. Chem. Res.* 2013, **46**, 2741.
2 S. Matile, A. Vargas Jentzsch, J. Montenegro, A. Fin, *Chem. Soc. Rev.* 2011, **40**, 2453.
3 T. M. Fyles, *Chem. Soc. Rev.* 2007, **36**, 335.
4 N. Sakai, S. Matile, *Langmuir* 2013, **29**, 9031–9040.
5 J. H. Fuhrhop, H. Hungerbuehler, U. Siggel, *Langmuir* 1990, **6**, 1295.
6 T. S. Arrhenius, M. Blanchard-Desce, M. Dvolaitzky, J. M. Lehn, J. Malthete, *Proc. Natl. Acad. Sci. USA* 1986, **83**, 5355.
7 M. Nango, T. Hikita, T. Nakano, T. Yamada, M. Nagata, Y. Kurono, T. Ohtsuka, *Langmuir* 1998, **14**, 407.
8 S.-I. Kugimiya, T. Lazrak, M. Blanchard-Desce, J.-M. Lehn, *J. Chem. Soc. Chem. Comm.* 1991, 1179.
9 L. E. Garner, J. Park, S. M. Dyar, A. Chworos, J. J. Sumner, G. C. Bazan, *J. Am. Chem. Soc.* 2010, **132**, 10042.
10 H. Hou, X. Chen, A. W. Thomas, C. Catania, N. D. Kirchhofer, L. E. Garner, A. Han, G. C. Bazan, *Adv. Mater. Weinheim* 2013, **25**, 1593.
11 L. E. Garner, A. W. Thomas, J. J. Sumner, S. P. Harvey, G. C. Bazan, *Energ. Environ. Sci.* 2012, **5**, 9449.
12 A. W. Thomas, L. E. Garner, K. P. Nevin, T. L. Woodard, A. E. Franks, D. R. Lovley, J. J. Sumner, C. J. Sund, G. C. Bazan, *Energ. Environ. Sci.* 2013, **6**, 1761.
13 B. E. Logan, *Nat Rev Micro* 2009, **7**, 375.
14 N. D. Kirchhofer, X. Chen, E. Marsili, J. J. Sumner, F. W. Dahlquist, G. C. Bazan, *Phys. Chem. Chem. Phys.* 2014, **16**, 20436.
15 J. Du, A. W. Thomas, X. Chen, L. E. Garner, C. A. Vandenberg, G. C. Bazan, *Chem. Commun.* 2013, **49**, 9624.
16 K. Sivakumar, V. B. Wang, X. Chen, G. C. Bazan, S. Kjelleberg, S. C. J. Loo, Bin Cao, *Appl. Microbiol. Biotechnol.* 2014, *98*, 9021.
17 J. Du, C. Catania, G. C. Bazan, *Chem. Mater.* 2014, **26**, 686.
18 J. Hinks, Y. Wang, W. H. Poh, B. C. Donose, A. W. Thomas, S. Wuertz, S. C. J. Loo, G. C. Bazan, S. Kjelleberg, Y. Mu, et al., *Langmuir* 2014, **30**, 2429.
19 A. W. Thomas, Z. B. Henson, J. Du, C. A. Vandenberg, G. C. Bazan, *J. Am. Chem. Soc.* 2014, **136**, 3736.
20 Y. Wang, Z. Zhou, J. Zhu, Y. Tang, T. D. Canady, E. Y. Chi, K. S. Schanze, D. G. Whitten, *Polymers* **2011**, **3**, 1199.
21 E. Quesada, A. U. Acuña, F. Amat-Guerri, *Angew. Chem. Int. Ed.* 2001, **40**, 2095.
22 W. W. Wilson, M. M. Wade, S. C. Holman, F. R. Champlin, *J. Microbiol. Meth.* 2001, **43**, 153.
23 A. L. Hillberg, M. Tabrizian, *Biomacromolecules* 2006, *7*, 2742.
24 Y. Wang, K. S. Schanze, E. Y. Chi, D. G. Whitten, *Langmuir* 2013, **29**, 10635.
25 M. Kahraman, A. I. Zamaleeva, R. F. Fakhrullin, M. Culha, *Anal. Bioanal. Chem.* 2009, **395**, 2559.
26 R. F. Fakhrullin, Y. M. Lvov, *ACS Nano* 2012, *6*, 4557.
27 A. J. Priya, S. P. Vijayalakshmi, A. M. Raichur, *J. Agr. Food Chem.* 2011, **59**, 11838.
28 D. M. Eby, S. Harbaugh, R. N. Tatum, K. E. Farrington, N. Kelley-Loughnane, G. R. Johnson, *Langmuir* 2012, **28**, 10521.
29 V. B. Wang, J. Du, X. Chen, A. W. Thomas, N. D. Kirchhofer, L. E. Garner, M. T. Maw, W. H. Poh, J. Hinks, S. Wuertz, S. Kjelleberg, Q. Zhang, J. S. C. Loo, and G. C. Bazan, *Phys. Chem. Chem. Phys.*, 2013, **15**, 5867.
30 C. E. Milliken, H. D. May, *Appl. Microbiol. Biotechnol.* 2006, **73**, 1180.
31 C. J. Sund, S. Mcmasters, S. R. Crittenden, L. E. Harrell, J. J. Sumner, *Appl. Microbiol. Biotechnol.* 2007, **76**, 561.
32 B. E. Logan, in *Microbial Fuel Cells*, John Wiley & Sons, Inc., Hoboken, 2008, pp. 4–6.
33 A. Herland, K. P. R. Nilsson, J. D. M. Olsson, P. Hammarström, P. Konradsson, O. Inganäs, *J. Am. Chem. Soc.* 2005, **127**, 2317.
34 A. Duarte, A. Chworos, S. F. Flagan, G. Hanrahan, G. C. Bazan, *J. Am. Chem. Soc.* 2010, **132**, 12562.
35 L. Cai, R. Zhan, K.-Y. Pu, X. Qi, H. Zhang, W. Huang, B. Liu, *Anal. Chem.* 2011, **83**, 7849.
36 T. Klingstedt, A. Aslund, R. A. Simon, L. B. G. Johansson, J. J. Mason, S. Nyström, P. Hammarström, K. P. R. Nilsson, *Org. Biomol. Chem.* 2011, **9**, 8356.
37 T. Klingstedt, C. Blechschmidt, A. Nogalska, S. Prokop, B. Haggqvist, O. Danielsson, W. K. Engel, V. Askanas, F. L. Heppner, K. P. R. Nilsson, *Chembiochem* 2013, **14**, 607.
38 K.-Y. Pu, K. Li, X. Zhang, B. Liu, *Adv. Mater.* 2010, **22**, 4186.

